Hybrid Molecular Materials Based upon Magnetic Polyoxometalates and Organic π-Electron Donors: Syntheses, Structures, and Properties of Bis(ethylenedithio)tetrathiafulvalene Radical Salts with Monosubstituted Keggin Polyoxoanions

Eugenio Coronado,* José R. Galán-Mascarós, Carlos Giménez-Saiz, Carlos J. Gómez-García, and Smaïl Triki†

Contribution from the Departamento de Química Inorgánica, Universidad de Valencia, Doctor Moliner 50, 46100 Burjasot, Spain

Received November 10, 1997

Abstract: The syntheses, crystal structures, and physical properties of the series of radical salts made with bis(ethylenedithio)tetrathiafulvalene (BEDT-TTF or ET) and monosubstituted α-Keggin polyoxoanions of formula $[XZ(H_2O)M_{11}O_{39}]^{5-}$ (XZM_{11} = $Si^{IV}Fe^{III}Mo_{11}$, $Si^{IV}Cr^{III}W_{11}$, $P^{V}Co^{II}W_{11}$, $P^{V}Ni^{II}W_{11}$, $P^{V}Cu^{II}W_{11}$ $P^{V}Zn^{II}W_{11}$, $P^{V}Mn^{II}W_{11}$, and $P^{V}Mn^{II}Mo_{11}$) containing a magnetic metal ion Z on a peripheral octahedral site of the Keggin anion are reported. They all crystallize in two related series called α_2 and α_3. The general structure consists of alternating layers of the organic donor and the Keggin polyoxometalates. While the stoichiometry and α-packing arrangement within the organic ET layers are the same in the two phases, significant differences are observed in the anion layers. Thus, in the α_3 phase the anions polymerize to form an unprecedented linear chain of Keggin anions along the *c* axis, while in the remaining compounds the anion layers are formed by discrete Keggin units. A salient feature of these structures is that in both phases the magnetic metal ion Z appears to be localized on two of the 12 possible octahedral sites of the monosubstituted Keggin anion, even if the Keggin anions are not bonded, as in the α_2 phase. The organic layers are formed by two different kinds of stacks: an eclipsed chain with almost totally ionized ET molecules and a dimerized one with partially charged ET molecules that accounts for the semiconducting character of these salts. Magnetic measurements of the radical salt with the diamagnetic Zn-containing Keggin anion indicate the presence of antiferromagnetic interactions in the organic sublattice ($|J| \approx 70$ cm^{-1}), together with a Curie tail at low temperatures, which has been attributed to a paramagnetic contribution coming from the progressive electron localization in the mixed-valence dimerized chain when cooling. All the salts having discrete magnetic anions (α_2 phase) show magnetic behaviors which correspond to the sum of the magnetic contributions of the two sublattices. This observation indicates that the interactions between the two sublattices are quite negligible, a result in agreement with the EPR measurements. However, with the two radical salts having chains of Keggin anions (α_3 phase: $PMnW_{11}$ and $PMnMo_{11}$) small differences between the ET and the tetrabutylammonium salts have been detected at low temperatures. In the [$PMnW_{11}$] derivative these differences have been attributed to single-ion effects. In the [$PMnMo_{11}$] derivative, these differences have been attributed to a weak antiferromagnetic Mn−Mn interaction promoted by the presence of a delocalized electron on the mixed-valence polyanion.

Introduction

A contemporary challenge in molecular chemistry is to design, from a wise choice of the constituent molecules, new materials that combine properties not normally associated with a single material.[1] Examples include hybrid molecular materials combining a magnetic component (typically an inorganic network containing transition metal ions) with an organic conducting component (typically formed by a π-electron donor or acceptor).[2] In this context the two main issues are (i) the creation of molecule-based materials with a coexistence of properties, in particular those possessing what might normally be considered to be mutually countermanding cooperative properties, such as *ferromagnetism and superconductivity*, and (ii) the preparation of molecular hybrids exhibiting a coupling between localized d-electrons with the conduction π-electrons (d-π interaction). In the former case the two networks must be quasi-independent, while in the second one non-negligible electronic interactions between the two networks are required. Such interaction may be able to couple the localized magnetic moments via an indirect exchange mechanism of the RKKY type[3] which involves the

† On leave from the Departement de Chimie, UMR 6521, Université de Bretagne Occidentale, BP 809, 29285 Brest, France.

(1) Day, P. *Philos. Trans. R. Soc. London* **1985**, *A314*, 145.

(2) See e.g.: Coronado, E.; Galán-Mascarós, J. R.; Giménez-Saiz, C.; Gómez-García, C. J. In *Magnetism: A Supramolecular Function*; Kahn, O., Ed.; NATO ASI Series C484; Kluwer Academic Publishers: The Netherlands, 1996; pp 281−298, and references therein.

(3) The indirect interaction which may occur in molecular systems differs from that occurring in the inorganic classical metals in the following points: (1) Most often the interaction between localized and conduction electrons is intermolecular, and thus weak, and involves a d-π exchange interaction, while in the inorganic metals this interaction is intra-atomic, and thus quite strong, and involves a direct interaction between localized 3d or 4f electrons and the delocalized conduction electrons (which are mainly of s character). (2) The electron correlation effects are much more important in the molecular metals than in the inorganic ones, and, therefore, the RKKY free electron model may be a too rude approach to account for the indirect exchange interactions in these hybrid molecular materials.

S0002-7863(97)03856-0 CCC: $15.00
Published on Web 05/02/1998

conduction electrons in a similar way to that proposed for explaining the ferromagnetism in some transition and rare earth metals and alloys.[4]

The most successful results have been found in cation radical salts formed by organic donor molecules of the tetrathiafulvalene type (in short TTF) and its derivatives with magnetic counterions. Thus, the first evidence for coexistence of localized and conduction electrons in a radical salt was observed in the $(ET)_3CuCl_4{\cdot}H_2O$ molecular metal (ET = bis(ethylenedithio)-tetrathiafulvalene).[5] A more striking example of such a coexistence is the $(ET)_4(H_2O)Fe(C_2O_4)_3{\cdot}C_6H_5CN$ radical salt (C_2O_4 = oxalate dianion), which combines superconductivity in a molecular organic lattice with magnetic moments localized on the anion complex.[6] On the other hand, a coupling between the two networks (d-π interaction) has been invoked in a few cases to justify the presence of weak interactions between the metal centers[7,8] or to account for the observation of unusual magnetic properties[9] or electrical phase transitions.[10]

Almost all the systems mentioned above contain very simple and small magnetic counterions, as for example the metal halide anions ($FeCl_4^-$, $CuCl_4^{2-}$, ...) or the tris-oxalate metal complexes ($Fe(C_2O_4)_3^{3-}$ and $Cr(C_2O_4)_3^{3-}$). However, more complex magnetic anions as the metal-oxide clusters of tungsten or molybdenum provided by the polyoxometalate chemistry can also be used as magnetic component of hybrid organic/inorganic materials having localized and delocalized electrons.[11] In fact, these soluble molecular metal oxides show the ability to accommodate one or several paramagnetic transition metal ions at specific sites of the polyoxoanion structure.[12] In addition to the magnetic character, the polyoxoanions possess other structural and electronic characteristics as their big sizes and shapes or the ability to accept one or more electrons which are fully delocalized over the polyoxoanion structure that make them suitable and attractive as an active counterion for new radical-cation salts.[13] The effect of the polyanion structure on the structure and electrical properties of these radical salts has been studied in more than 40 radical salts of organic donors with various diamagnetic polyoxometalates with metal nuclearities of 6 (Lindqvist $[M_6O_{19}]^{2-}$; M = W^{VI}, Mo^{VI}),[14] 8 (β-octamolybdate $[Mo_8O_{26}]^{4-}$),[15] 12 (α-Keggin $[XW_{12}O_{40}]^{(8-n)-}$ (X^{n+} = P^V, Si^{IV}),[16] and 18 (Dawson-Wells $[P_2W_{18}O_{62}]^{6-}$).[17] On the other hand, the electron acceptor character of the polyanion $[PMo_{12}O_{40}]^{3-}$ has given rise to radical salts with coexistence of delocalized electrons on the two molecular sublattices.[18] Very recently we have started to exploit the ability of the polyoxoanion to bear a localized magnetic moment. As magnetic polyoxoanions we have used α-Keggin anions having a magnetic ion (Co^{II}, Cu^{II} and Fe^{III}) in the central tetrahedral site[19] and the anions $[M_4(PW_9O_{34})_2]^{10-}$ which contain a tetrameric magnetic cluster M_4O_{16} (M^{2+} = Co, Mn)[20] with ferromagnetic or antiferromagnetic pairwise interactions, respectively. The most significant result has been the discovery of an extensive family of radical salts formulated as $(ET)_8[XW_{12}O_{40}]{\cdot}(solv)_n$ (X = $2H^+$, B^{III}, Si^{IV}, Co^{II}, Cu^{II}, Fe^{III}).[19] These semiconducting magnetic materials are the first example of polyoxometalate-containing radical salts with coexistence of localized and delocalized electrons. No sizable interaction between the two sublattices has been detected in these systems down to 2 K, in agreement with the good insulation of the central magnetic site provided by the Keggin structure. A way to increase this interaction is to bring the magnetic moments localized on the anions nearer to the π-electrons placed on the organic sublattice. To explore this possibility we have used the family of monosubstituted polyoxoanions formulated as $[X^{n+}Z^{m+}(H_2O)M_{11}O_{39}]^{(12-n-m)-}$ (X = P^V, Si^{IV}; M = Mo^{VI}, W^{VI}; Z = Fe^{III}, Cr^{III}, Mn^{II}, Co^{II}, Ni^{II}, Cu^{II}, and Zn^{II}) (abbreviated as $[XZM_{11}]$) that can be considered as derived from the nonsubstituted Keggin anions $[X^{n+}M_{12}O_{40}]^{(8-n)-}$ (abbreviated as $[XM_{12}]$) by simply replacing one of the external constituent atoms, M, and its terminal oxygen atom by a transition metal atom, Z, and a water molecule, respectively. From the similarity in charge, shape, and size it can be anticipated that the structures of the radical salts obtained with the monosubstituted polyanions $[XZM_{11}]$ will be quite similar to those obtained with the nonsubstituted $[XM_{12}]$ polyanions. The present paper reports the syntheses, crystal structures, and physical properties of the two related series of radical salts obtained from the magnetic

(4) (a) Elliott, J. R. *Magnetism*; Rado & Suhl, Eds.; Academic Press: New York, 1965, *IIA*, p 385. (b) Mott, N. F. *Metal*−*Insulator Transitions*; Taylor & Francis: London, 1990. (c) For a detailed description of the exchange interactions in molecular materials, including the RKKY one, see also: Coronado, E.; Georges, R.; Tsukerblat, B. In *Molecular Magnetism: From Molecular Assemblies to the Devices*; Coronado, E., Delhaes, P., Gatteschi, D., Miller, J. S., Eds.; NATO ASI Series E321; Kluwer Academic Publishers: The Netherlands, 1996; p 65.

(5) Day, P.; Kurmoo, M.; Mallah, T.; Marsden, I. R.; Friend, R. H.; Pratt, F. L.; Hayes, W.; Chasseau, D.; Gaultier, J.; Bravic, G.; Ducasse, L. *J. Am. Chem. Soc.* **1992**, *114*, 10722.

(6) Kurmoo, M.; Graham, A. W.; Day, P.; Coles, S. J.; Hursthouse, M. B.; Caulfield, J. L.; Singleton, J.; Pratt, F. L.; Hayes, W.; Ducasse, L. Guionneau, P. *J. Am. Chem. Soc.* **1995**, *117*, 12209.

(7) Kumai, R.; Asamitsu, A.; Tokura, Y. *Chem. Lett.* **1996**, 753.

(8) Coronado, E.; Falvello, L. R.; Galán-Mascarós, J. R.; Giménez-Saiz, C.; Gómez-García, C. J.; Lauhkin, V. N.; Pérez-Benítez, A.; Rovira, C.; Veciana, J. *Adv. Mater.* **1997**, *9*, 984.

(9) Almeida, M.; Gama, V.; Henriques, R. T.; Alcácer, L. In *Inorganic and Organometallic Polymers with Special Properties*; Laine, R. M., Ed.; Kluwer Academic Publishers: The Netherlands, 1992; pp 163−177.

(10) Kobayashi, H.; Tomita, H.; Naito, T.; Kobayashi, A.; Sakai, F.; Watanabe, T.; Cassoux, P. *J. Am. Chem. Soc.* **1996**, *118*, 368.

(11) (a) Coronado, E.; Gómez-García, C. J. *Comments Inorg. Chem.* **1995**, *17*, 255. (b) Coronado, E.; Delhaes, P.; Galán Mascarós, J. R.; Giménez-Saiz, C.; Gómez-García, C. J. *Synth. Met.* **1997**, *85*, 1647. (c) Coronado, E.; Gómez-García, C. J. *Chem. Rev.* **1998**, *98*, 273.

(12) (a) Pope, M. T. *Heteropoly and Isopoly Oxometalates*; Springer-Verlag: Berlin, 1983. (b) Pope, M. T.; Müller, A. *Angew. Chem., Int. Ed. Engl.* **1991**, *30*, 34. (c) Coronado, E.; Gómez-García, C. J. In *Polyoxometalates: From Platonic Solids to Anti-Retroviral Activity*; Pope, M. T., Müller, A., Eds.; Kluwer Academic Publishers: The Netherlands, 1994; pp 233−243.

(13) Ouahab, L. *Chem. Mater.* **1997**, *9*, 1909.

(14) (a) Bellitto, C.; Attanasio, D.; Bonamico, M.; Fares, V.; Imperatori, P.; Patrizio, S. *Mater. Res. Soc. Proc.* **1990**, *173*, 143. (b) See: Ouahab, L. In *Polyoxometalates: From Platonic Solids to Anti-Retroviral Activity*; Pope, M. T., Müller, A., Eds.; Kluwer Academic Publishers: The Netherlands, 1994; pp 245. (c) Coronado, E.; Galán Mascarós, J. R.; Giménez-Saiz, C.; Gómez-García, C. J.; Rovira, C.; Tarrés, J.; Triki, S.; Veciana, J. *J. Mater. Chem.* **1998**, *8*, 313.

(15) (a) Gómez-García, C. J.; Coronado, E.; Triki, S.; Ouahab, L.; Delhaes. P. *Synth. Met.* **1993**, *56*, 1787. (b) Gómez-García, C. J.; Coronado, E.; Triki, S.; Ouahab, L.; Delhaes, P. *Adv. Mater.* **1993**, *5*, 283.

(16) (a) Ouahab, L.; Bencharif, M.; Grandjean, D. *C. R. Acad. Sci. Paris, Série II* **1988**, *307*, 749. (b) Ouahab, L.; Bencharif, M.; Mhanni, A.; Pelloquin, D.; Halet, J. F.; Peña, O.; Padiou, J.; Grandjean, D.; Garrigou-Lagrange, C.; Amiell, J.; Delhaès, P. *Chem. Mater.* **1992**, *4*, 666. (c) Davidson, A.; Boubekeur, K.; Pénicaud, A.; Auban, P.; Lenoir, C.; Batail, P.; Hervé, G. *J. Chem. Soc. Chem. Commun.* **1989**, 1373. (d) Bellitto, C.; Bonamico, M.; Staulo, G. *Mol. Cryst. Liq. Cryst.* **1993**, *232*, 155.

(17) Coronado, E.; Galan-Mascaros, J. R.; Gimenez-Saiz, C.; Gomez-Garcia, C. J.; Laukhin, V. N. *Adv. Mater.* **1996**, *8*, 801.

(18) Bellitto, C.; Bonamico, M.; Fares, V.; Federici, F.; Righini, G.; Kurmoo, M.; Day, P. *Chem. Mater.* **1995**, *7*, 1475.

(19) (a) Gómez-García, C. J.; Ouahab, L.; Giménez-Saiz, C.; Triki, S.; Coronado, E.; Delhaès, P. *Angew. Chem., Int. Ed. Engl.* **1994**, *33*, 223. (b) Gómez-García, C. J.; Giménez-Saiz, C.; Triki, S.; Coronado, E.; Le Magueres, P.; Ouahab, L.; Ducasse, L.; Sourisseau, C.; Delhaès, P. *Inorg. Chem.* **1995**, *34*, 4139.

(20) (a) Gómez-García, C. J.; Borrás-Almenar, J. J.; Coronado, E.; Delhaes, P.; Garrigou-Lagrange, C.; Baker, L. C. W. *Synth. Met.* **1993**, *56*, 2023. (b) Clemente-León, M.; Coronado, E.; Galán-Mascarós, J. R.; Giménez-Saiz, C.; Gómez-García, C. J.; Otero, T. F. *J. Mater. Chem.* **1998**, *8*, 309.

Table 1. Unit Cell Parameters for the Series of Radical Salts α_2-$ET_8[XZ(H_2O)M_{11}O_{39}]$ (XZM_{11} = $SiFeMo_{11}$, $SiCrW_{11}$, $PZnW_{11}$, $PCoW_{11}$, $PCuW_{11}$ and $PNiW_{11}$), and α_3-$ET_{8n}[PMnM_{11}O_{39}]_n$ (M = W and Mo)

salt[a]	*a* (Å)	*b* (Å)	*c* (Å)	β (deg)	*V* (Å^3)
$\alpha_2-ET_8[SiFeMo_{11}]$[b]	16.55(3)	43.261(7)	12.12(1)	111.2(1)	8093
$\alpha_2-ET_8[SiCrW_{11}]$[b]	16.490(4)	43.195(5)	12.152(5)	111.31(2)	8064
$\alpha_2-ET_8[PNiW_{11}]\cdot 2H_2O$[c]	16.599(7)	43.373(8)	12.121(5)	111.78(5)	8103
$\alpha_3-ET_{8n}[PMnW_{11}]_n\cdot 2nH_2O$[c]	19.927(5)	43.384(7)	11.199(5)	123.06(3)	8114
$\alpha_3-ET_{8n}[PMnMo_{11}]_n$[b]	19.90(2)	43.20(2)	11.191(7)	123.32(6)	8041

[a] For the α_2-$ET_8[PZnW_{11}]$, α_2-$ET_8[PCoW_{11}]$, and α_2-$ET_8[PCuW_{11}]$ salts, due to the small amount of sample available, it was only possible to perform a Guinier-type X-ray diffractogram to confirm the isostructurality with the other salts of the α_2 series. [b] Unit cell parameters determined from single crystals. [c] Compounds whose structures have been fully determined from single-crystal X-ray diffraction.

polyoxometalates [XZM_{11}] and the organic donor ET. While the stoichiometry and packing arrangement within the organic ET layers are the same in all the compounds, significant differences are observed in the anion layers. Thus in the two compounds containing $[PMnM_{11}]^{5-}$ (M = W, Mo), this anion polymerizes to form an unprecedented linear chain of Keggin anions sharing an oxo bridge, while in the remaining compounds the anion layers are formed by discrete Keggin units. From the electronic point of view, no interactions between the localized d electrons and the itinerant π electrons are detected down to 2K. A preliminary account of the Keggin chain structure has already been published.[21]

Experimental Section

Synthesis of the Radical Salts. All the radical salts were obtained on a platinum wire electrode by anodic oxidation of the organic donor ET ($\approx 2 \times 10^{-3}$ M in a 1:2 mixture of CH_3CN/CH_2Cl_2 or $CHCl_2-CH_2Cl$) in a U-shaped electrocrystallization cell under low constant current (I = 0.6−1.2 μA) in the presence of the tetrabutylammoniun (NBu_4^+) salts of the polyanions ($\approx 10^{-2}$ M in a 1:1 mixture of CH_3CN/CH_2Cl_2) as supporting electrolyte. The solvents were not previously dried. In fact, in most cases the addition of some drops of water (up to 1 mL) in the anode was necessary to obtain good quality single crystals, suggesting that either the water or the protons (or both) are necessary for the crystallization of the salts. All the crystals were collected, washed with CH_3CN and CH_2Cl_2 (to remove any portion of neutral ET or the NBu_4^+ salts of the polyanions), and air-dried. The NBu_4^+ salts of the polyanions were prepared following the methods described below. The purity of all these NBu_4^+ salts was checked and confirmed by their IR spectra, magnetic measurements, and in one case with its single-crystal X-ray structure (in the salt $(NBu_4)_4H[SiCr(H_2O)W_{11}O_{39}]$). It is noteworthy that for the Mo salts the magnetic moments were smaller than the expected values (up to 10−15%), indicating the existence of some nonmagnetic impurity, which, possibly, may be attributed to the monovacant Keggin anion [PMo_{11}] or to the reconstituted Keggin anion [PMo_{12}]. However, during the electrocrystallization process only the monosubstituted anion is incorporated in the radical salt structure, as demonstrated by the magnetic measurements.

Preparation of $(NBu_4)_4H[SiCr(H_2O)W_{11}O_{39}]$. The salt α-$K_8[SiW_{11}O_{39}]\cdot 13H_2O$ (37 g), prepared by the method of Tézé and Hervé,[22] was dissolved in 200 mL of distilled water at 90 °C, and 4.65 g of $Cr(NO_3)_3\cdot 9H_2O$ was added. Once dissolved the $Cr(NO_3)_3\cdot 9H_2O$, the solution was allowed to cool at room temperature, and the pH of this dark green solution was adjusted to 4.7 by addition of small portions of sodium acetate. NBu_4Br (18.7 g) was added in order to precipitate the NBu_4^+ salt of the $[SiCr(H_2O)W_{11}O_{39}]^{5-}$ anion. The so obtained green precipitate was collected, washed with water, ethanol, and ether, dried in air, and recrystallized twice in dimethylformamide (DMF) to obtain dark green cubic-shaped crystals of the salt $(NBu_4)_4H[SiCr(H_2O)W_{11}O_{39}]$.

Preparation of $(NBu_4)_4H[SiFe(H_2O)Mo_{11}O_{39}]$. This salt was prepared following the method of Petit and Massart,[23] but using NBu_4-Br to precipitate the polyanion as the NBu_4^+ salt. The so obtained yellow precipitate was collected, washed with water and ethanol, dried in air, and recrystallized twice in CH_3CN to obtain yellow cubic-shaped crystals of the salt $(NBu_4)_4H[SiFe(H_2O)Mo_{11}O_{39}]$.

Preparation of $(NBu_4)_4H[PMn(H_2O)Mo_{11}O_{39}]$. This salt was prepared with a modification of the method of Fournier:[24] A solution of 32.5 g of $(NH_4)_6Mo_7O_{24}\cdot 4H_2O$ in 166 mL of distilled water was cooled to 0 °C. The pH of this solution was adjusted to 4.5−5.0 with acetic acid (aproximately 3 mL were needed). A pale pink solution prepared with 83.4 mL of H_3PO_4 0.2 M, 33 mL of H_2SO_4 0.5 M, and 16.7 mL of $MnSO_4\cdot H_2O$ 1 M was added to the paramolybdate solution. The polyanion $[PMn(H_2O)Mo_{11}O_{39}]^{5-}$ was immediately precipitated as the NBu_4^+ salt by the addition of an excess of solid NBu_4Br. This brown solid was immediately collected, washed with cold water, dried in air, and recrystallized twice in DMF to obtain brown hexagonal prismatic crystals of the salt $(NBu_4)_4H[PMn(H_2O)Mo_{11}O_{39}]$.

Preparation of $(NBu_4)_4H[PZ(H_2O)W_{11}O_{39}]$ (Z^{II} = Mn, Co, Ni, Cu, and Zn). All these salts were prepared by the same method.[21] The transition metals were added either as acetates, nitrates, or sulfates. All the solids were collected, washed with water, ethanol, and ether, dried in air, and recrystallized twice in CH_3CN to obtain red-wine (Z = Co^{II}), pale green (Z = Ni^{II}), pale blue (Z = Cu^{II}), pale brown (Z = Mn^{II}), and white (Z = Zn^{II}), well formed single crystals of the NBu_4^+ salts.

X-ray Crystallography. The unit cell parameters and orientation matrix for data collection were obtained from least-squares refinement, using the setting angles of the first 25 reflections found for each crystal (see Table 1). The X-ray crystal structures were determined for the salt which gave the best quality crystals of each structural type: α_2-$ET_8[PNi(H_2O)W_{11}O_{39}]\cdot 2H_2O$ and α_3-$ET_{8n}[PMnW_{11}O_{39}]n\cdot 2nH_2O$. The crystals, which are stable in air, were mounted on an Enraf-Nonius CAD4 diffractometer equipped with a graphite crystal, incident beam monochromator. Preliminary examination and data collection were performed with Mo Kα radiation. During data collection three standard reflections were measured every hour and showed no significant decay. Lorentz, polarization, and a semiempirical absorption correction (ψ-scan method)[25] were applied to the intensity data. Other important features of the crystal data are summarized in Table 2. Among the three possible monoclinic space groups,[26] *I*2, *Im*, and *I*2/*m*, corresponding to the extinction conditions, the latter was retained on the basis of the successful solution and refinement of the structures. All calculations were performed on a VAX computer using MolEN.[27] The structures were solved by direct methods using MULTAN[28] and were developed with successive full-matrix least-squares refinements and difference Fourier syntheses, which showed all the atoms of organic donors, the polyanion, and the solvent molecules. On the contrary to the ET molecules, which show no evident crystallographic disorder, the Keggin anions in the α_2 phase appear as centrosymmetric units as a result of disorder due to rotation of 90° around the C_2 axis of the central

(21) Galán-Mascarós, J. R.; Gimenez-Saiz, C.; Triki, S.; Gómez-García, C. J.; Coronado, E.; Ouahab, L. *Angew. Chem., Int. Ed. Engl.* **1995**, *34*, 1460.
(22) Tézé, A.; Hervé, G. *J. Inorg. Nucl. Chem.* **1977**, *39*, 999.
(23) Petit M.; Massart, R. *C. R. Acad. Sc. Paris* **1969**, *268*, 1860.
(24) Fournier, M. *C. R. Acad. Sci. Sér. C*, **1971**, *273*, 1569.
(25) North, A. C. T.; Philips, D. C.; Mathews, F. S. *Acta Crystallogr., Sect. A* **1968**, *24*, 351.
(26) *International Tables for Crystallography*; Hahn, T., Ed.; D. Reidel Pub. Co.: 1983; Vol A (Space Group Symmetry).
(27) MolEN, *An Interactive Structure Solution Procedure*; Enraf-Nonius: Delft, The Netherlands, 1990.
(28) Main, P.; Germain, G.; Woolfson, MULTAN-11/84, *a System of Computer Programs for the Automatic Solution of Crystal Structures from X-ray Diffraction Data*; University of York: 1984.

Table 2. Crystal Data for the Salts α_2-$ET_8[PNi(H_2O)W_{11}O_{39}]\cdot 2H_2O$ (**I**) and α_3-$ET_8[PMnW_{11}O_{39}]\cdot 2H_2O$ (**II**)

	I	**II**
chemical formula	$C_{80}H_{68}S_{64}PNiW_{11}O_{42}$	$C_{80}H_{68}S_{64}PMnW_{11}O_{41}$
formula weight	5865.54	5845.77
crystal system	monoclinic	monoclinic
space group	*I*2/*m* (no. 5)	*I*2/*m* (no. 5)
unit cell parameters	$a = 16.599(7)$ Å	$a = 19.927(5)$ Å
	$b = 43.373(8)$ Å	$b = 43.384(7)$ Å
	$c = 12.121(5)$ Å	$c = 11.199(5)$ Å
	$\beta = 111.78(5)°$	$\beta = 123.06(3)°$
volume	8103(7) Å^3	8114(7) Å^3
Z	2	2
ρ calc	2.404 g cm^{-3}	2.392 g cm^{-3}
absorption coeff	89.25 cm^{-1}	88.71 cm^{-1}
T	22 °C	22 °C
λ	0.71069 Å	0.71069 Å
2Θ range	2.03−49.84°	2.14−51.92°
reflections collected	7610	8171
$I > n\sigma(I)$	3.0	5.0
data/parameters	2302/307	3165/309
goodness-of-fit	1.525	1.374
R^a	0.062	0.046
$R_w{}^b$	0.078	0.064

^{a} $R = \sum[|F_o| - |F_c|]/\sum|F_o|$. ^{b} $R_w = [\sum\omega(|F_o| - |F_c|)^2/\sum\omega|F_o|^2]^{1/2}$, $\omega = 4F_o^2/[\sigma^2(I) + (0.07|F_o|^2)^2]$.

tetrahedron. This kind of disorder has been found in other crystal structures with Keggin anions surrounded by big and weakly polarizing cations[29] as clearly described and explained by Pope and Evans.[30] A direct consequence of this disorder is the impossibility of refining all the oxygen atoms of the anion with anisotropic thermal parameters. Nevertheless, the reliability factors are in the normal range found for other polyoxometalate salts.[31]

A noticeable fact found in both structures is the location of the magnetic centers (Z = Ni or Mn) in only two opposite positions of the 12 possible locations in the Keggin anion. Thus, of the six crystallographically independent W atoms, five could be refined as W atoms, whereas the other could only be refined assuming a mixed atom W/Z with an occupancy factor that converged to a value of 0.5 for each metal.

Magnetic Measurements. Variable temperature susceptibility measurements were carried out in the temperature range 2−300 K at a magnetic field of 0.1 T on polycrystalline samples with a magnetometer (Quantum Design MPMS-XL-5) equipped with a SQUID sensor. The susceptibility data were corrected from the diamagnetic contributions of the ET molecules (-201.6×10^{-6} emu·mol^{-1} per ET molecule, as deduced by using Pascal's constant tables) and from the diamagnetic and TIP contributions of the Keggin units (these contributions were calculated from the susceptibility measurements of the NBu_4^+ salts of the corresponding Keggin anions and are similar to those applied in other radical salts of TTF with Keggin polyanions). Variable-temperature ESR spectra of single crystals were recorded at X-band with a Bruker ER200 spectrometer equipped with a helium cryostat. The field was measured using a diphenylpicrylhydrazyl (DPPH, g = 2.0036) stable free radical marker.

IR and UV−vis Spectroscopies. IR spectra were recorded in the range 400−4700 cm^{-1} on pressed KBr pellets with a Perkin-Elmer 882 FT-IR spectrophotometer. UV−vis spectra were recorded at room temperature on pressed KBr pellets with a Perkin-Elmer 330 UV−vis spectrophotometer in the range 3850−25000 cm^{-1}.

Results and Discussion

Crystal Structures of α_2-$ET_8[PNi(H_2O)W_{11}O_{39}]\cdot 2H_2O$ (1) and α_3-$ET_{8n}[PMnW_{11}O_{39}]_n\cdot 2nH_2O$ (2). A total of eight ET radical salts were synthesized with monosubstituted Keggin anions [XZM_{11}] showing the general stoichiometry 8:1. They exhibit two different monoclinic structures as demonstrated by their unit cell parameters (see Table 1), namely α_2 and α_3. Only the structures of the α_2-Ni^{II} and α_3-Mn^{II} derivatives were solved as they were the ones that gave better quality single crystals. These structures are related to those obtained for the 8:1 ET radical salts containing nonsubstituted Keggin anions [XM_{12}], which crystallize in two structures namely α_1 and α_2.[19b] In fact, the α_2 structure is common to both kinds of radical salts.

The structures of these two phases consist of alternating layers of the organic donors and the inorganic Keggin anions perpendicular to the *b* axis (Figure 1). As for the organic component, it should be noticed that the change of a nonsubstituted Keggin anion by a monosubstituted one does not affect the structural features of this component. Thus, as in the previous cases, the organic layers are formed by two different types of stacks (named I and II in Figure 1) running in the [101] direction and alternating in the [10$\bar{1}$] direction. Stack II is formed by eclipsed ET molecules, whereas stack I consists of eclipsed dimers packed bond-to-ring with the neighboring dimers giving rise to a zigzag chain of dimers. In both kinds of chains the ET molecules are tilted with respect to the packing direction (typical of the α phases) in such a way that the ET molecules of neighboring stacks form an angle of about 46°. On the other hand, the interstack distances are significantly shorter than the intrastack ones, as in many other two-dimensional radical salts of ET.[32] In fact, the shortest interchain S−S contacts range from 3.41(2) to 3.46(2) Å, whereas the intrachain ones range from 3.79(2) Å to 3.86(1) Å and from 3.89(2) to 4.00(2) Å in the zigzag stacks (for intra- and interdimer distances, respectively) and from 3.98(2) to 4.04(2) Å in the eclipsed stacks. Another important feature of these structures is the presence of short contacts between the organic and the inorganic layers. Thus, two kinds of interactions can be observed: (1) between the S atoms of the eclipsed chains and some terminal O atoms of the polyoxoanions (shortest S−O distances ranging from 3.01(2) to 3.22(2) Å) and (2) via hydrogen bonds between several O atoms of the anions and the ethylenic groups of the ET molecules (shortest C−O distances ranging from 2.98(3) to 3.13(3) Å).

In the organic part the only noticeable difference between the two phases is the number of crystallographically independent ET molecules. Thus, the α_2 phase is formed by two distinct ET molecules (noted as A and B; there are four ET molecules of each type per anion), whereas the α_3 phase possesses three distinct ET molecules (noted as A, B, and C; there are four ET molecules of type A, two of type B, and two of type C per anion). Consequently, in the α_2 phase the eclipsed chain (type

(29) (a) Sergienko, V. S.; Porai-Koshits, M. A.; Yurchenko, E. N. *J. Struct. Chem. (Engl. Transl.)* **1980**, *21*, 87. (b) Fuchs, J.; Thiele, A.; Palm, R. *Angew. Chem., Int. Ed. Engl.* **1982**, *21*, 789. (c) Attanasio, D.; Bonamico, M.; Fares, V.; Imperatori, P.; Suber, L. *J. Chem. Soc., Dalton Trans.* **1990**, 3221.

(30) Evans, H. T.; Pope M. T. *Inorg. Chem.* **1984**, *23*, 501.

(31) (a) Weakley, T. J. R.; Evans, H. T.; Showell, J. S.; Tourné, G. F.; Tourné, C. M. *J. Chem. Soc., Chem. Commun.* **1973**, 139. (b) Robert, F.; Leyrie, M.; Hervé, G. *Acta Crystallogr.* **1982**, *B38*, 358. (c) Knoth, W. H.; Domaille, P. J.; Harlow, R. L. *Inorg. Chem.* **1986**, *25*, 1577. (d) Evans, H. T.; Tourné, G. F.; Tourné, C. M.; Weakley, T. J. R. *J. Chem. Soc., Dalton Trans.* **1986**, 2699. (e) Wasfi, S. H.; Rheingold, A. L.; Kokoszka, G. F.; Goldstein, A. S. *Inorg. Chem.* **1987**, *26*, 2934. (f) Finke, R. G.; Rapko, B.; Weakley, T. J. R. *Inorg. Chem.* **1989**, *28*, 1573. (g) Weakley, T. J. R.; Finke, R. G. *Inorg. Chem.* **1990**, *29*, 1235. (h) Tourné, C. M.; Tourné, G. F.; Zonnevijlle, F. *J. Chem. Soc., Dalton Trans.* **1991**, 143. (i) Gómez-García, C. J.; Coronado, E.; Gómez-Romero, P.; Casañ-Pastor, N. *Inorg. Chem.* **1993**, *32*, 3378. (j) Gómez-García, C. J.; Borrás-Almenar, J. J.; Coronado, E.; Ouahab, L. *Inorg. Chem.* **1994**, *33*, 4016. (k) Finke, R.; Weakley, T. J. R. *J. Chem. Crystal.* **1994**, *24*, 123.

(32) Williams, J. M.; Ferraro, J. R.; Thorn, R. J.; Carlson, K. D.; Geiser, U.; Wang, H. H.; Kini, A. M.; Whangbo M. H. *Organic Superconductors. Synthesis, Structure, Properties and Theory;* Crimes, R. N., Ed.; Prentice Hall: Englewood Cliffs, NJ, 1992.

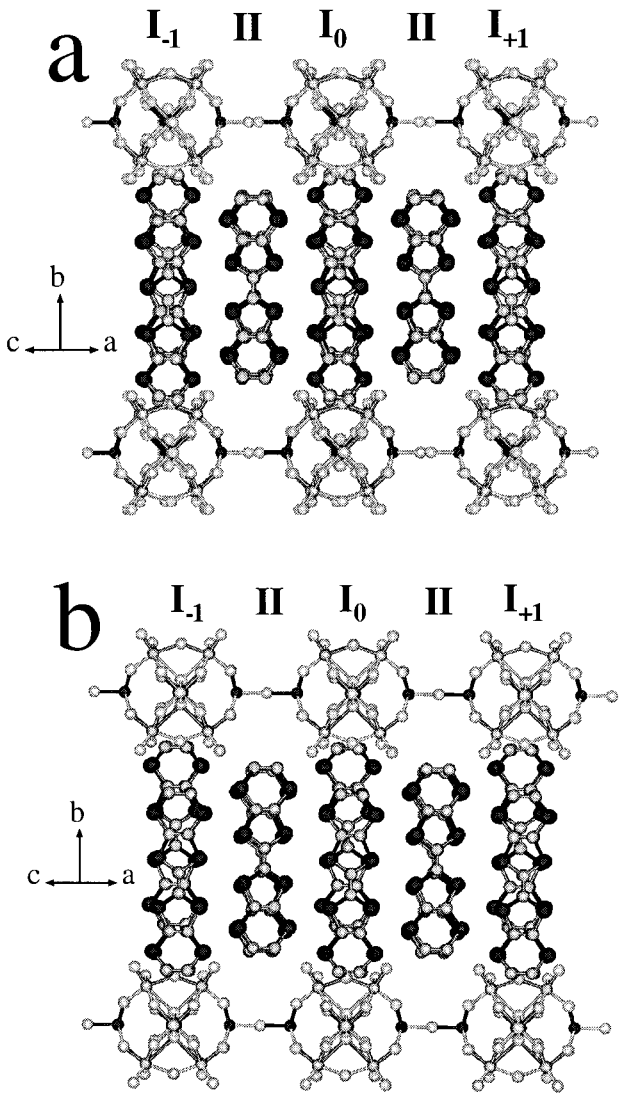

Figure 1. (a) Structure of the α_2-$ET_8[PNi(H_2O)W_{11}O_{39}]\cdot 2H_2O$ radical salt showing the alternating layers of the polyanions and the organic donors and the two different types of organic chains I and II. The dark atom in the periphery of the anions indicate the two possible locations of the Ni atoms. (b) Structure of the α_3-$ET_{8n}[PMnW_{11}O_{39}]_n\cdot 2nH_2O$ radical salt showing the alternating layers of the polyanions and the organic donors and the two different types of organic chains I and II. Note the common oxygen atom that bridges the W/Mn atoms (in dark).

II) is formed by the B-type molecules, whereas in the α_3 phase this chain is formed by alternated B and C-type molecules. In both α phases the dimerized chain (type I) is exclusively formed by the A-type molecules. It should be noted that, in this aspect, the α_3 phase is identical to the α_1. The charges on these different ET molecules can be very roughly estimated using the known correlations between the bond distances of the TTF skeleton and the degree of ionicity of the ET molecules.[33] As for the other known phases, the crystallographic data indicate that in both phases those molecules forming the eclipsed chain are almost completely ionized, whereas the molecule forming the dimerized chain is rather neutral.[34] In view of the stoichiometry of this series (8:1) and of the anion charge (−5), this analysis suggests that one electron is delocalized over the four ET molecules of the dimerized chain (giving an average charge of 1/4 per molecule), while the remaining four electrons are localized on the four ET molecules of the eclipsed chain.

The inorganic part exhibits in both phases striking structural features which are unprecedented in polyoxometalate chemistry. The most significant one is the formation of chains of Keggin anions connected by an oxo-bridge, as observed in the α_3 phase. A second feature that is common to both phases is the partial localization of the external metal heteroatom, Z, over two of the 12 possible octahedral sites of the monosubstituted Keggin anion. This ordering is quite difficult to detect by X-ray diffraction studies since, in most of the Keggin salts, e.g., with NBu_4^+ or alkaline cations, these anions impose a high cubic symmetry for the crystal packing. The metal atom Z, then, appears to be fully disordered over the 12 metal sites[12a,35] even when the anion is not located on a special position.[36] What is surprising in this respect is that this metal ion ordering is found not only when the Keggin units are forming a chain (α_3 phase) but also when they are isolated (as in the α_2 phase). In the following we will discuss in detail these results.

Let us focus first our attention on the α_3 phase. Two opposite octahedral sites of the undecatungsto complex of Mn^{2+} are connected by a common oxo-bridge forming a linear chain of Keggin anions running along the *c* axis (Figure 1b). These two positions are occupied by W and Mn atoms with an occupancy factor 0.5. This fact implies that the Mn^{2+} ion is delocalized between these two special positions (called Mn/W). It is important to notice that such a partial disorder is merely statistical and results from the two possible chain orientations in the crystal lattice (in half of the chains the Mn atom is on the left side of the Keggin unit, while in the other half this is on the right part). Actually, each oxo-bridge always connects a W atom with a Mn one giving rise to an ordered sequence Mn−O−W within the chain (there are no W−O−W nor Mn−O−Mn bridges, as will be seen from the magnetic properties below). In fact, from the chemical point of view, the only way to form a chain of monosubstituted Keggin units implies the displacement of the terminal water molecule coordinated to Mn in one Keggin unit by a terminal oxygen atom from a W of the neighboring Keggin anion, with the subsequent formation of a bridge Mn−O−W connecting the two anions.

An additional consequence of the formation of the anion chains is the elongation of the Keggin structure in the chain direction. Such a distortion, observed for the first time in the present case thanks to the low symmetry of the crystal (monoclinic), can be evaluated from the P−metal distances which change from 3.54 to 3.57 Å (for the ten P−W distances) to 3.63 Å (for the two P−(Mn/W) distances). Soon after the publication of this structure,[21] Weakley et al. published the structure of the NEt_4^+ salt of the $[PCoW_{11}]^{5-}$ anion,[37] where a similar Keggin chain is present. Nevertheless, in the Weakley's compound the Keggin units are not distorted, and the two possible positions for the Co atom are not equivalent, as indicated by the different metal−O_{bridge} bond distances (1.84 and 2.00 Å) and by the occupancy factor of the Co atom in

(33) (a) Umland, T. C.; Allie, S.; Kuhlmann, T.; Coppens, P. *J. Phys. Chem.* **1988**, *92*, 6456. (b) Guionneau, P.; Kepert, C. J.; Bravic, G.; Chasseau, D.; Truter, M. R.; Kurmoo, M.; Day, P. *Synth. Met.* **1997**, *86*, 1973.

(34) Although the standard deviations in the bond distances are very high in all the structures, the estimated charges on each ET molecule are very close to zero (0.0−0.3) for those of the dimerized chain (A-type) and much higher (0.5−1.0) for those of the eclipsed chain (types B in the α_2 phase and B and C in the α_3 phase).

(35) (a) Baker, L. C. W.; Baker, V. S.; Eriks, K.; Pope, M. T.; Shibata, M.; Rollins, O. W.; Fang, J. J.; Koh, L. L. *J. Am. Chem. Soc.* **1966**, *88*, 2329.

(36) Sergienko, V. S.; Porai-Koshits, M. A. *Zh. Neorg. Khim.* **1985**, *30*, 2282; *Russ. J. Inorg. Chem. (Engl. Transl.)* **1985**, *30*, 1297.

(37) Evans Jr., H. T.; Weakly, T. J. R.; Jameson, G. B. *J. Chem. Soc., Dalton Trans.* **1996**, 2537.

these two positions (0.39 and 0.61, respectively). The absence/presence of distortions in the Keggin anions can be related with the differences in the intermolecular interactions between the organic counterions. In our salt the high tendency of the ET molecules to form parallel stacks with strong intermolecular π interactions and short distances must, in a way, have some influence on the packing and therefore on the distortions of the Keggin units. On the contrary, the cations NEt_4^+ have not this tendency, and, moreover, they are able to adopt different conformations to overcome the steric restrictions imposed by the Keggin chains. In fact, in the $[PCoW_{11}]$ derivative, the ethyl groups of the cations are completely disordered, suggesting that they do not impose any distortion to the polyanions.

Focusing now on the α_2 phase, we observe that the Ni^{2+} ion is located on two opposite octahedral sites of the monosubstituted anion $[PNi(H_2O)W_{11}O_{39}]^{5-}$. As in the α_3 phase, these two positions are occupied by W and Ni atoms with an occupancy factor 0.5. To understand this supramolecular ordering we have compared the differences in the dimensionality of the anion layer when passing from the α_1 to the α_2 and to the α_3 phases. In Figure 2 we have examined the two closest distances between the two terminal oxygen atoms of neighboring Keggin polyanions. Thus, in the α_1 phase the shortest distances in the two directions of layer, namely d1 and d2, are very close (d1 $\approx$ d2 $\approx$ 6.0 Å), while in the α_2 and phase α_3 phases, d2 remains almost constant (d2 $\approx$ 6.2 Å) but d1 decreases significantly from 3.7 Å in α_2 to zero in α_3. These changes indicate a reduction in the dimensionality of the anionic network from the two-dimensional α_1 phase to the one-dimensional α_3 phase, with the α_2 phase adopting an intermediate dimensionality.

From the structural results we notice that the $[PNi(H_2O)W_{11}O_{39}]^{5-}$ anions are oriented in such a way that the sites occupied by the Ni^{2+} ions are those involving the closest oxygen−oxygen distance, d1 $\approx$ 3.7 Å. This means that intermolecular interactions along the *c* direction are at the origin of this particular orientation of the clusters. As possible interactions we can consider the presence of hydrogen bonds between the water molecule coordinated to the Ni and a terminal oxo group belonging to a W atom of the neighboring anion. However, the d1 distance is too large to afford this kind of interaction. Another possibility comes from the electrostatic repulsion between these two oxygens. Simple electrostatic arguments predict that this repulsion should be smaller for a Ni site−W site pair than for a W site−W site pair: In the former case the interaction takes place between a negatively charged oxo group of an anion and the water molecule coordinated to Ni of the nearest neighbor anion, while in the later it involves a repulsion between two negatively charged oxo groups of neighboring anions. This electrostatic argument provides a simple explanation to the preferential occupation of the Ni sites predicting also an ordering of the anions similar to that assumed in the one-dimensional α_3 phase with the Keggin anions having the same orientation within each array. From the above results it is clear that the formation of a chain of Keggin anions is not a necessary condition to have an ordered arrangement of these kind of anions in the crystal lattice. This order can also occur for salts containing discrete monosubstituted Keggin anions when they adopt anisotropic packings in the solid state.

An additional question deserving to be posed is why these significant differences in the inorganic packings among the three crystalline α-phases do not affect the organic packings, which remain nearly unchanged for the three phases. We can answer to this question noticing that a simple structural relationship

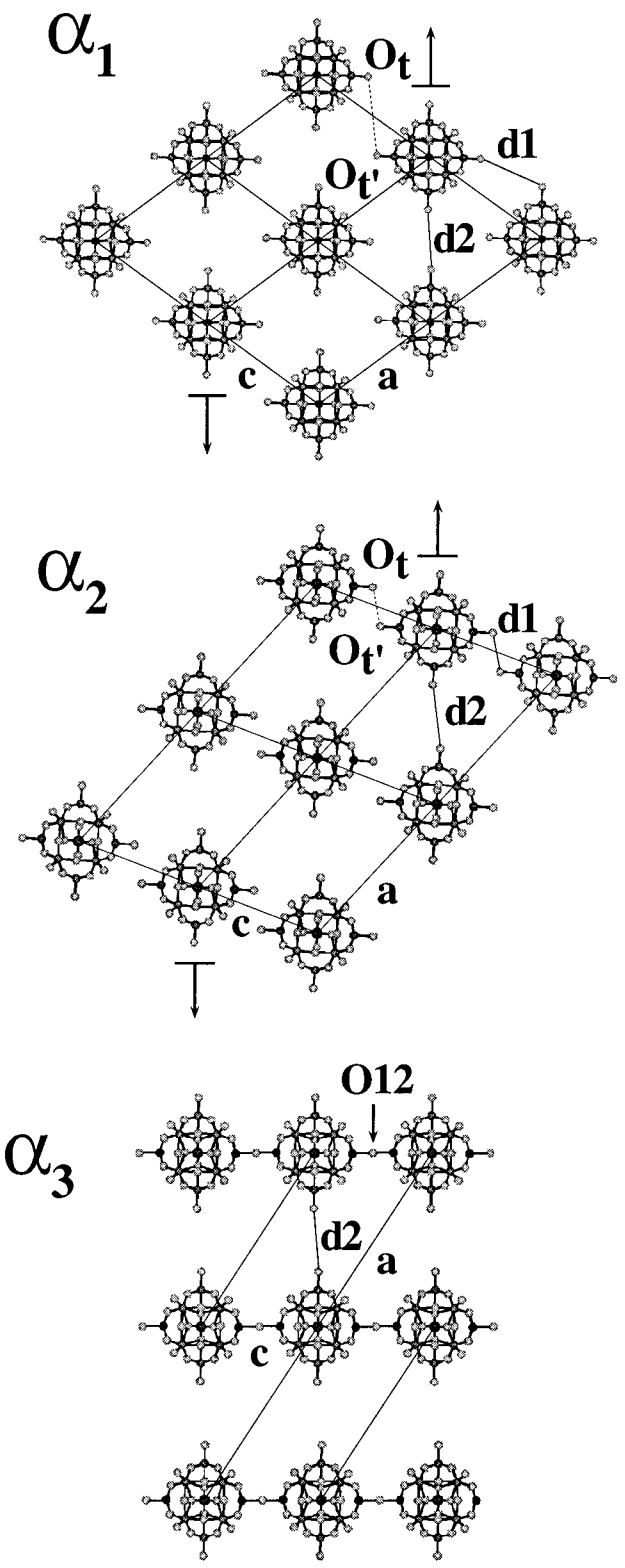

Figure 2. Structure of the inorganic layers in the three α series showing the displacements suffered by the anions and the changes in the closest anion−anion distances in the two directions (d1 and d2). O_t and $O_{t'}$ indicate the terminal oxygen atoms that close up and converge in the bridging oxygen O12 in the α_3 series.

relates the three phases. As can be seen in Figure 3a the α_1 phase can be converted to the other two phases by displacing in opposite directions the dimerized stacks I_{+1} and I_{-1} by one or two intrastack ET-ET distances ($\Delta \approx 4$ Å), the eclipsed stacks (type II) remaining fixed.[38] Since these displacements are in fact along the stacking axis (direction [101]), this process

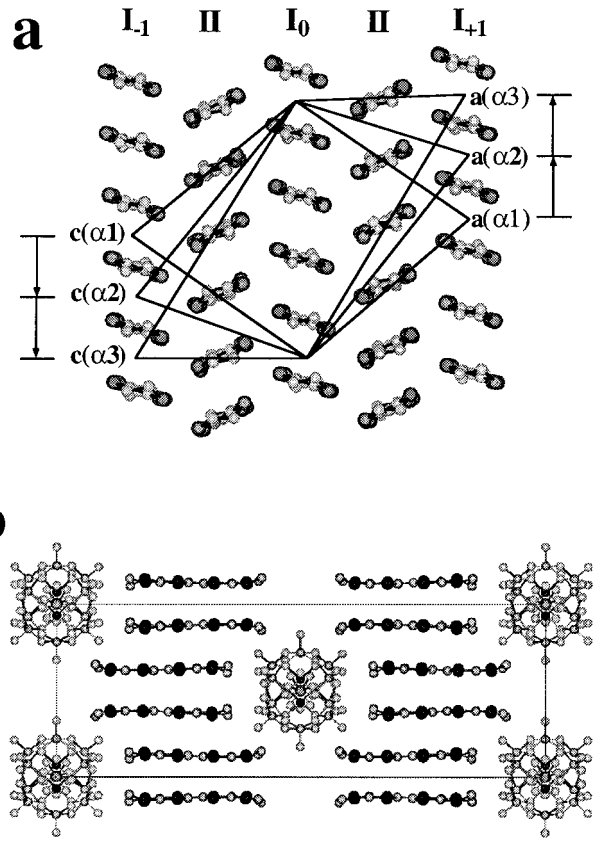

Figure 3. (a) View of the organic layer in the ac plane for the three α series showing the displacements suffered by the organic molecules of type I chains. (b) Side view of the type I chains showing the zigzag ET dimers and the holes occupied by the anions.

changes the relative situation of the chains, but the interchain ET distances and the packing within the chains remain practically invariant. As the polyoxometalates lie in the holes left by two dimerized stacks of consecutive layers (Figure 3b), they must accompany the organic displacements. Therefore, a shortening of the distances between terminal oxygen atoms of neighboring Keggin units along the *c* direction occurs. This accounts for the significant changes observed in the dimensionality of these inorganic layers.

Finally, when comparing the series of monosubstituted salts $[XZM_{11}]$ and the nonsubstituted $[XM_{12}]$ series, there are some structural differences worth mentioning: (i) Each monosubstituted Keggin anion always leads to a single crystalline phase. This fact contrasts with the $[XM_{12}]$ anions which often crystallizes in both the α_1 or α_2 phases, depending on the synthetic conditions (except for $[SiW_{12}]$ and $[BW_{12}]$). (ii) of the many $[XZM_{11}]$ polyanions used, only those with an anionic charge of -5 ($[PZ^{II}M_{11}]$ and $[SiZ^{III}M_{11}]$ anions) give ET salts. In turn, radical ET salts of the nonsubstituted anions have been obtained with anion charges comprised between -4 and -6. (iii) The change of W by Mo does not produce any change in the resulting structure, as has been observed in the two radical salts with the α_3 structure. In contrast, for the nonsubstituted Keggin polyanions, the only known example ($[PM_{12}]$) has shown a drastic change in the structure when changing W by Mo.[39] (iv) In the monosubstituted salts only the Mn derivatives give rise to the α_3 structure showing a chain of Keggin anions, while the salts with the remaining anions show the α_2 structure, where the anion sublattice is formed by discrete Keggin units. Such a difference may be related with the bigger ionic radius of the Mn^{2+} ion compared to those of the remaining 3d metal ions (Z = Cr^{3+}, Fe^{3+}, Co^{2+}, Ni^{2+}, Cu^{2+}, and Zn^{2+}). In the case of manganese, its bigger size facilitates the formation of the oxo bridge between the elongated Keggin units of the polymer chain. The difference between the $[PMnM_{11}]$ complexes (M = W and Mo) and the other monosubstituted Keggin anions is only observed in the solid-state radical salts. In the precursor NBu_4^+ salts of these polyanions, the $[PMnM_{11}]$ complexes are present as discrete units as in the other members of the series $[XZM_{11}]$. In fact, all these NBu_4^+ salts are isostructural exhibiting a cubic lattice with $a = 17.6-17.7$ Å. Probably in nonaqueous solution the polyanions are also present as discrete species, and only when the lattice is being formed do the Mn complexes polymerize.

Optical and Transport Properties. The IR spectra of the salts are all very much alike, confirming the presence of the same type of stacks in all the salts, except in the 1000−400 cm^{-1} region where small differences, due to the different polyanions, are observed. In all the spectra the electronic A band (corresponding to electronic transfers between neutral and completely charged ET molecules)[40] is observed as a large and intense band centered at 4000−5000 cm^{-1}, indicating the existence of a mixed-valence state in the organic donors. The main band wavenumbers and their assignments[41] for both the ET molecules and the anions are listed in the Supporting Information. In general, the bands of the ET molecules are very similar to those found in other completely ionized ET^+ radical cations,[41c] suggesting the presence of almost completely charged ET molecules. Nevertheless, the additional presence of almost neutral ET molecules cannot be inferred from the IR spectra as these ET molecules would give rise to very weak bands[42] for the modes characteristic of the degree of ionicity (ν_2, ν_3, and ν_{27}). The only significant differences in the IR spectra, as expected, come from the M−O (M = Mo, W), X−O (X = Si, P) and Z−O (Z = Cr, Fe, Mn, Co, Ni, Cu, and Zn) bonds.

The electrical properties of this series, measured on single crystals,[43] show that these salts are semiconductors with room-temperature conductivities of $10^{-1}-10^{-2}$ S·cm^{-1} and thermal activation energies $E_a = 100-150$ meV. This behavior is quite analogous to that observed in the nonsubstituted Keggin series, in agreement with the similar donor packing in all these crystal phases.

Magnetic properties: The α_2 Series. We will first focus on the $ET_8[PZnW_{11}]$ salt, as it is the only one to have a diamagnetic anion which can enable us to study the magnetic behavior of the organic layer. The static magnetic susceptibility of the $[PZnW_{11}]$ salt exhibits a shoulder in χ_m around 60 K and a paramagnetic Curie tail at lower temperatures (Figure 4). The plot of the $\chi_m T$ product vs *T* shows a continuous decrease on

(38) The relationship between the three α phases clearly indicates that no more possible α phases may be generated in the same way, as a further movement of Δ from the α_3 phase will lead to the α_1 phase (notice that the centrosymmetric dimers may only have three different relative positions in the stack).

(39) The radical salt of ET with the $[PMo_{12}]$ anion presents the α_1 structure (see ref 18), whereas that with the [PW12] anion presents a completely different structure and stoichiometry (3:1) (see ref 14b).

(40) Torrance, J. A.; Scot, B. A.; Welber, F. B. *Phys. Rev B* **1979**, *19*, 730.

(41) The assignment have been made following the nomenclature of (a) Swietlik, R.; Garrigou-Lagrange, C.; Sourisseau, C.; Pages, G.; Delhaes, P. *J. Mater. Chem.* **1992**, *2*, 857, with the interpretations of (b) Maceno, G. Ph.D. Thesis, Bordeaux, France, **1988** and (c) Kozlov, M. E.; Pokhodnia, K. I.; Yurchenko, A. A. *Spectrochim. Acta* **1989**, *45A*, 437.

(42) Moldenhauer, J.; Horn, Ch.; Pokhodnia, K. I.; Schweitzer, D.; Heinen, I.; Keller, H. J. *Synth. Met.* **1993**, *60*, 31.

(43) Owing to the small size of the crystals, conductivity measurements were performed using a two-probe method.

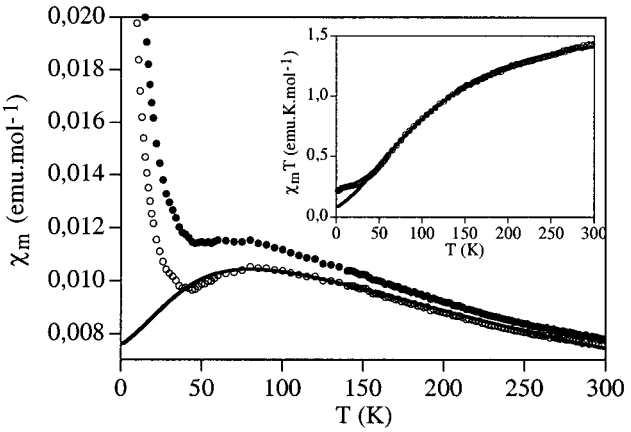

Figure 4. Plot of the molar susceptibility (filled circles) and the Curie-tail corrected susceptibility (open circles) versus temperature for the radical salt α_2-$ET_8[PZn(H_2O)W_{11}O_{39}]$. Inside: plot of the product of the molar susceptibility times the temperature versus temperature for the same compound. Solid lines are the best fit to the model (see text).

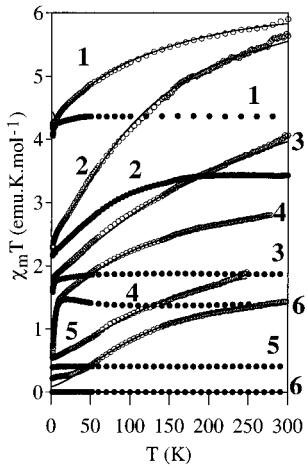

Figure 5. Plot of the product of the molar susceptibility times the temperature versus temperature for the series of radical salts α_2-$ET_8[XZ(H_2O)M_{11}O_{39}]$, XZM_{11} = $SiFeMo_{11}$ (**1**), $SiCrW_{11}$ (**2**), $PCoW_{11}$ (**3**), $PNiW_{11}$ (**4**), $PCuW_{11}$ (**5**), and $PZnW_{11}$ (**6**) (open circles) and for the NBu_4^+ salts of the same anions (closed circles). Solid lines are the best fit to the model (see text).

lowering the temperature from a value of about 1.5 emu·K·mol^{-1} to a value around 0.2 emu·K·mol^{-1}, indicating an antiferromagnetic coupling between the ET molecules (inset in Figure 4). This behavior resembles that observed in the radical salts with the diamagnetic Keggin polyanions $[H_2W_{12}]$, $[SiW_{12}]$, and $[BW_{12}]$.[19b] In view of the close structural and electronic similarities of the organic layers in all the α phases we can apply the model previously used to fit the magnetic behavior of these radical salts. This model assumes three different magnetic contributions coming from (i) a fully localized regular chain formed by completely ionized ET molecules with spins $S = 1/2$ antiferromagnetically coupled through an exchange, J_1; (ii) a delocalized mixed-valence dimerized one with a singlet-to-triplet gap, J_2, accounting for an activated magnetic term; and (iii) a small amount of isolated spins accounting for the observed Curie tail at low temperatures. In this simple model this last contribution comes from the small number of spins present in the dimerized chain, which becomes progressively localized and therefore mostly isolated as the temperature is lowered.

If we subtract to the experimental data a Curie contribution ($C = 0.08$ emu·K·mol^{-1}) so that the experimental maximum in χ_m matches that of a regular antiferromagnetic chain, we obtain an excellent agreement with the model at $T > 30$ K (Figure 5). In this fit we have assumed, according with the charge distribution, that the localized eclipsed chain is completely ionized ($n_1 = 4$), while the four ET molecules in the dimerized chain bear a charge of 1/4 ($n_2 = 1$, where n_1 and n_2 are the number of spins per formula in the eclipsed and dimerized chains, respectively). The resulting magnetic exchange parameters obtained for the eclipsed chain ($J_1 = -71$ cm^{-1}) and the dimerized one ($J_2 = -280$ cm^{-1}) are close to those found in the $[XM_{12}]$ radical salts[19b] and are summarized in Table 3. On the other hand, J_1 is in the range of values observed in other radical salts.[44] Below 30 K the applied paramagnetic correction appears not to be enough as the susceptibility diverges and moves away from the theoretical behavior. This discrepancy suggests that the magnetic component of the organic sublattice is not as simple as it has been supposed. In fact, the model considers two independent types of chains neglecting the possible interchain interactions, while the transfer integrals obtained with theoretical band calculations indicate that the organic lattice has a strong two-dimensional character.[19b] The electronic delocalization effects are also neglected by the model. A more elaborated model that takes these effects into account, in particular the influence of the interaction of the localized π-electrons of the antiferromagnetic chain with the delocalized π-electrons of the mixed-valence chain, is under way.

Table 3. Magnetic Parameters for the Series of Radical Salts α_2-$ET_8[XZ(H_2O)M_{11}O_{39}]$ (XZM_{11} = $SiFeMo_{11}$, $SiCrW_{11}$, $PZnW_{11}$, $PCoW_{11}$, $PCuW_{11}$, and $PNiW_{11}$) and α_3-$ET_{8n}[PMnM_{11}O_{39}]_n$ (M = W and Mo)

salt	C (emu/mol)	$-J_1$ (cm^{-1})	$-J_2$ (cm^{-1})
α_2-PZnW_{11}	0.080	72	280
α_2-PCoW_{11}	0.214	84	350
α_2-PCuW_{11}	0.130	84	350
α_2-PNiW_{11}	0.160	70	350
$\alpha_2-SiFeMo_{11}$	0	84	350
$\alpha_2-SiCrW_{11}$	0.100	70	350
$\alpha_3-PMnMo_{11}$	0	90	350
α_3-PMnW_{11}	0.100	84	280

The magnetic behavior of those radical salts containing magnetic anions are shown in Figure 5 as the product of the magnetic susceptibility times temperature ($\chi_m T$) vs the temperature and compared with those of the corresponding NBu_4^+ salts. For all these salts, the magnetic moment (proportional to the square of the $\chi_m T$ product) decreases with decreasing temperature to reach, at low T, the value corresponding to the magnetic Keggin anions. This feature indicates that both sublattices do not interact significantly, despite the fact that short contacts between the organic and inorganic parts are present in the structure and that now the magnetic sites are on the surface of the Keggin anion instead of being insulated in the central site of the anion (as in the $[XM_{12}]$ series). In fact, once the magnetic moments of the different anions are subtracted, the contribution of the organic sublattice is very similar to that obtained in the $[PZnW_{11}]$ salt and can be fitted from similar values for J_1 and J_2 (Table 3).

More precise information on this point is provided by ESR measurements performed at helium temperature. In all cases, the spectra show a narrow signal centered at $g \approx 2$ with line widths in the range 25−40 G coming from the ET radicals,

(44) (a) Laversanne, R. Ph.D. Thesis, Bordeaux, France, 1987. (b) Obertelli, S. D.; Friend, R. H.; Talham, D. R.; Kurmoo, M.; Day, P. *J. Phys.: Condens. Matter* **1989**, *1*, 5671.

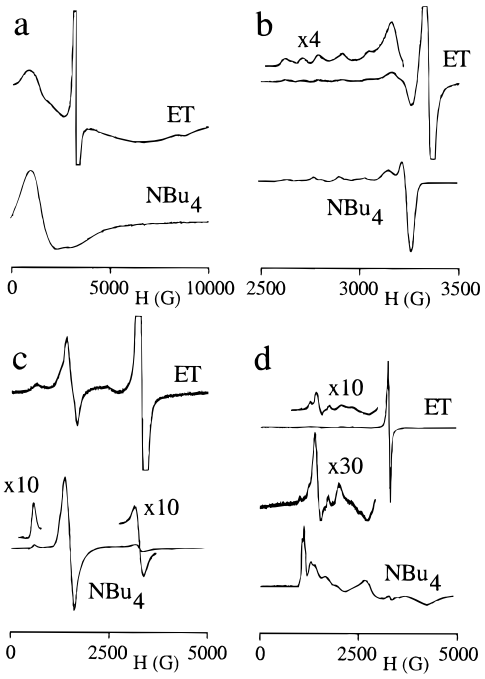

Figure 6. EPR spectra at 4.2 K of the series of radical salts $ET_8[XZ(H_2O)W_{11}O_{39}]$ and of the NBu_4^+ salts of the same anions: (a) XZ = PCo^{II}, (b) XZ = PCu^{II}, (c) XZ = $SiFe^{III}$ and (d) XZ = $SiCr^{III}$.

plus the characteristic signals of the magnetic anions (see Figure 6). These signals closely match those observed in the NBu_4^+ salts of the corresponding paramagnetic anions. In some cases, they even show hyperfine structures and zero-field splitting effects specific to the single ions. From these results we can conclude that the exchange interactions between the two sublattices are quite negligible. A possible reason to explain this lack of magnetic exchange interactions lies in the fact that the distances between the magnetic metal sites and the ET molecules, although shorter than in the $[XM_{12}]$ series, are still too long[45] to afford the way for an effective d-π interaction. In fact, the octahedral sites where the magnetic ions are located are those furthest away from the ET molecules (see Figure 1).

The α_3 Series. As already mentioned in the description of the structures, the main difference between α_2 and α_3 phases is that in the last, the Keggin anions are no longer discrete entities but linked ones sharing an oxygen atom to form chains with Mn−O−M (M = W or Mo) bonds. This change in the inorganic sublattice does not affect the organic one that maintains its structural and electronic properties.

The magnetic behavior of the radical salt with the $[PMnW_{11}]$ anion is displayed in Figure 7a and is compared with that of the NBu_4^+ salt of the same anion. At first sight, the magnetic behavior resembles those of the α_2-radical salts: the $\chi_m T$ product decreases with decreasing temperature and reaches, a low T, the value of the anion (as observed from its NBu_4^+ salt). This result may indicate that, as in the previous series, both sublattices are magnetically independent. In fact, the organic contribution may be fitted with similar parameters to those obtained in the α_2 series (see Table 3). However, a close inspection of the data in the low-temperature region (Figure 7b) allows one to observe that the magnetic moment of the ET salt crosses the

(45) The shortest metal−ET distances in the α_2 (Ni−C = 5.17 Å and Ni−S = 6.26 Å) and α_3 series (Mn−C = 5.01 Å and Mn−S = 6.23 Å) are much longer than the shortest metal−BET distances (Fe−C = 3.88 Å and Fe−S = 4.27 Å) in the $BET_2[FeCl_4]$ salt (BET = bis(ethylenethio)−tetrathiafulvalene), where weak exchange interactions have been observed between the Fe^{III} ions: see ref 8.

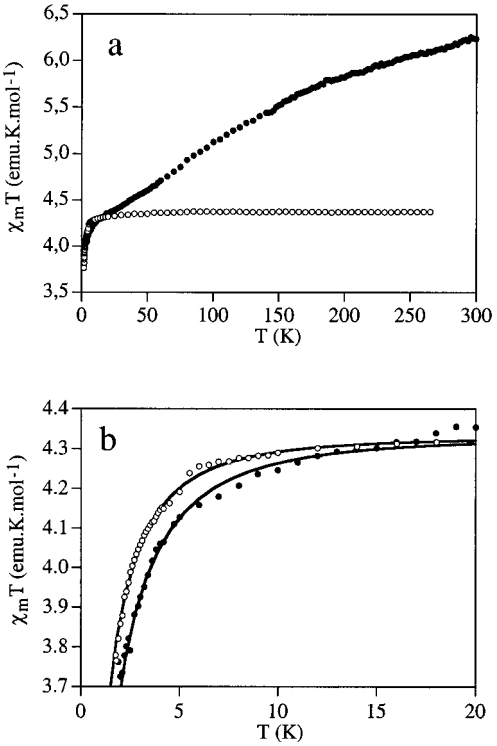

Figure 7. (a) Plot of the product of the molar susceptibility times the temperature versus temperature for the radical salt α_3-$ET_{8n}[PMnW_{11}O_{39}]_n \cdot 2nH_2O$ (closed circles) and for the NBu_4^+ salt of the same anion (open circles). (b) Low T region of this plot. The solid lines represent the best fit to the model (see text).

curve of the NBu_4^+ salt below 15 K. This result may be indicative of a very weak, although detectable, antiferromagnetic exchange interaction between the Mn^{2+} ions via the π-conducting electrons (indirect exchange interaction). The lack of interactions in the α_2 series (where the metal−ET distances are very similar) makes it hard to accept such an explanation, and, consequently, other possibilities that should be related with the distinctive structural features of the α_3 phase have to be explored. In this respect, the two reasons that may be at the origin of the observed behavior are (i) the presence of antiferromagnetic interactions Mn−Mn within the Keggin chain via a superexchange mechanism or a dipolar coupling and (ii) the presence of a single ion anisotropy due to the distortion of the Mn octahedral site. The possibility of a superexchange mechanism involving Mn^{2+} ions of adjacent Keggin units is not very realistic as the exchange pathway would imply a −O−P−O−W−O− bridge that seems to be too long to produce the observed effect. The dipolar coupling should also have a negligible effect in view of the long distance between the magnetic centers (the shortest Mn−Mn distance is 11.2 Å).

As far as the single ion anisotropy is concerned, we may expect different zero field splitting values for the Mn^{2+} when comparing the ET salt with the NBu_4^+ salt, due to the different distortions in the Mn^{2+} environment. Thus, in the ET salt, the Mn site is forced to have a large axial distortion in order to form the chain of Keggin anions, while in the NBu_4^+ salt such distortion is expected to be smaller since the Keggin anions are present as discrete entities. In fact, such differences can be seen by comparing the coordination environment of the Mn^{2+} ion in the $[PMnW_{11}]$ chain with that of the Ni^{2+} ion in the discrete $[PNiW_{11}]$ Keggin units that are forming the ET radical salt.[46] Thus, when passing from a discrete Keggin anion to a Keggin chain a significant elongation of the octahedral site is observed (Figure 8). The axial metal−oxygen distances $Z-O_P$

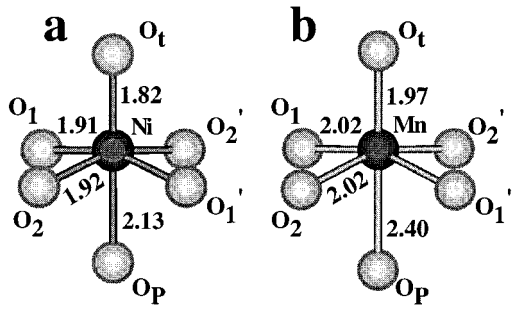

Figure 8. Coordination polyhedra of the Ni^{2+} and Mn^{2+} ions in the radical salts α_2-$ET_8[XNi(H_2O)W_{11}O_{39}]\cdot 2H_2O$ and α_3-$ET_{8n}[PMnW_{11}O_{39}]_n\cdot 2nH_2O$ showing the distortions in the Mn−O_t and Mn−O_P distances.

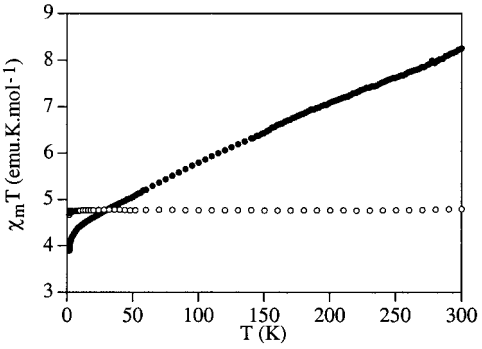

Figure 9. Plot of the product of the molar susceptibility times the temperature versus temperature for the radical salt α_3-$ET_{8n}[PMnMo_{11}O_{39}]_n\cdot 2nH_2O$ (closed circles) and for the NBu_4^+ salt of the same anion (open circles).

and Z−O_b increase by 0.27 and 0.15 Å (O_P is the oxygen atom linked to the central P atom and O_b is the oxo bridge), while the equatorial ones only increase by 0.1 Å which corresponds to the increase in the ionic radii when passing from Ni^{2+} (0.78 Å) to Mn^{2+} (0.91 Å). Such axial elongation should modify the zero field splitting of the Mn^{2+} ion, which is expected to be larger in the chain compound than in the NBu_4^+ salt, and therefore the magnetic properties of the two salts. In fact, the differences observed in the low temperature behavior can be quantitatively explained in terms of a change in the zero field splitting parameter D that increases from 1.25 cm^{-1} in the NBu_4^+ salt to 1.60 cm^{-1} in the ET salt (solid lines in Figure 7b).

The magnetic behavior of the radical salt with the $[PMnMo_{11}]$ anion is shown in Figure 9. For this anion the $\chi_m T$ product of the ET salt continuously decreases with decreasing T, but, in contrast with all the other radical salts, the $\chi_m T$ product of the ET salt crosses the curve of the NBu_4^+ salt and remains clearly below at $T < 30$ K. Moreover, if we look at the $\chi_m T$ value of the NBu_4^+ salt, we can observe that its value is ca. 4.75 emu·K·mol^{-1} at high T, a value higher than that of the NBu_4^+ salt of the related anion $[PMnW_{11}]$ (ca. 4.3 emu.K.mol^{-1}). This result suggests that the $[PMnMo_{11}]$ anion must be reduced by one electron, as has been observed in many other polyoxomolybdates.[12,47] The reduction of the Mo polyanion can be easily checked from the low-temperature ESR spectra of the NBu_4^+ salt. In Figure 10 the Mo and W polyanions EPR spectra are compared. As we can see, the spectrum of the Mo-containing anion shows, besides the low field signals between 500 and 2000 G corresponding to the Mn^{2+} ion in a distorted octahedral environment, an anisotropic signal centered at $g \approx 2$, characteristic of the reduced polyanion.[47,48]

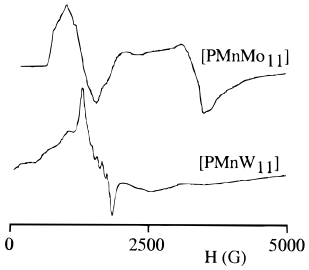

Figure 10. EPR spectra at 4.2 K of the NBu_4^+ salts of the polyanions $[XMn(H_2O)M_{11}O_{39}]$ (M = Mo and W) showing the features of the Mn^{II} ion in both spectra and of the reduced electron, only in the Mo derivative.

When the ET salt of this anion is formed, we can suppose that the Keggin anions remain reduced, giving rise to a chain of mixed-valence Keggin anions in which the localized magnetic moments coming from the Mn^{2+} ion coexist with delocalized "blue" electrons. As the general structure of this salt is the same that the one of the W anion, a magnetic interaction between the two sublattices is not expected. Thus, the crossing observed in Figure 9 must be related with the presence of delocalized electrons on the Mo anions. A possible explanation may be the existence of an antiferromagnetic exchange between the Mn^{2+} ions which now can be coupled via the delocalized electrons of the mixed-valence Keggin chain. This effect may be reinforced by the better ability of Mo compared to W in transmitting interactions between magnetic centers as has been recently shown in other polyoxomolybdate clusters.[49] Notice that reduced Keggin polyanions containing localized magnetic centers are already known.[50] They provide nice examples to study at the molecular level the coupling between localized and delocalized electrons. In this context the mixed-valence Keggin chain reported here may provide a unique opportunity to study this problem in one-dimension.

Conclusions

We have reported in this paper an extensive new series of hybrid radical salts formed by the organic donor bis(ethylenedithio)tetrathiafulvalene and Keggin polyoxoanions having magnetic centers in their surface. From the structural point of view, the new compounds exhibit quite unexpected structural features which are *unprecedented in polyoxometalate chemistry*.

(i) The most significant one is the formation of linear chains of Keggin anions $[PMnM_{11}]$ connected by an oxo-bridge in the *c* direction. With the remaining anions a related structure with the same α-packing mode in the organic layers is obtained, but the Keggin anions are no longer forming chains but layers of discrete anions with a marked anisotropy in the *c* direction.

(46) Since it is not possible to know the exact structural features of the Mn site in the NBu_4^+ salt because it appears to be fully disordered over the 12 metal sites, we assume that in the monosubstituted Keggin anions the environment of Ni^{2+} and Mn^{2+} are very similar, independently of the counterions (NBu_4^+ or ET). Thus, the structure of the nickel containing ET salt will be used to get information on the distortions of the Z site in the monosubstituted Keggin anions.

(47) Barrows, J. N.; Pope, M. T. *Adv. Chem. Ser.* **1990**, *226*, 403.

(48) (a) Prados, R. A.; Pope, M. T.; *Inorg. Chem.* **1976**, *15*, 2547. (b) Sánchez, C.; Livage, J.; Launay, J. P.; Fournier, M.; Jeannin, Y. *J. Am. Chem. Soc.* **1982**, *104*, 3194. (c) Pope, M. T. *Prog. Inorg. Chem.* **1991**, *39*, 181.

(49) Gatteschi, D.; Sessoli, R.; Plass, W.; Müller, A.; Krickemeyer, E.; Meyer, J.; Sölter, D.; Adler, P. *Inorg. Chem.* **1996**, *35*, 1926.

(50) (a) Casañ-Pastor, N.; Baker, L. C. W. *J. Am. Chem. Soc.* **1992**, *114*, 10384. (b) Casañ-Pastor, N.; Baker, L. C. W. In *Polyoxometalates: From Platonic Solids to Anti-Retroviral Activity*; Pope, M. T., Müller, A., Eds.; Kluwer Academic Publishers: The Netherlands, 1994; p 203.

(ii) The second novel feature is that in the two structures (α_2 and α_3) the magnetic metal ions Z have been crystallographically localized on two of the 12 possible octahedral sites of the monosubstituted Keggin anion. Such orientation of the anions along the *c* direction is not surprising in the chain structure (α_3 phase) since its formation requires the presence of Mn−O−W bridges connecting the Keggin units. What is surprising is to find also this orientation in the α_2 phase since, in contrast with the α_3 phase, the Keggin anions are no longer connected but independent. The above result emphasizes the importance of weak intermolecular interactions, other than the hydrogen bondings, in determining the supramolecular architecture of an anisotropic solid. On the other hand, it demonstrates that in order to have an ordered arrangement of the substituted Keggin anions in the crystal lattice, the formation of a chain of Keggin units is not a necessary requirement.

As far as the intermolecular electronic interactions are concerned, an important point deserving attention concerns the magnetic interactions within and between the two constituent networks. In all these organic/inorganic molecular hybrids the common electronic feature is the *coexistence of localized and itinerant electrons*. However, depending on the compound different kinds of electronic arrangement are possible. The most simple case occurs when a nonmagnetic anion is used as an inorganic component (i.e., the $[PZnW_{11}]$ derivative), since then only the organic part is electronically active. As for the ET salts with nonsubstituted Keggin anions, such a system behaves as an antiferromagnetic uniform chain with localized electrons on π-orbitals and a mixed-valence dimerized chain where the itinerant electrons reside. The fact that the low T magnetic behavior is not simply the sum of these two spin components may be due to the presence of a magnetic interaction between the two kinds of π-electrons ($\pi-\pi$ interaction).

When paramagnetic ions are introduced into the polyanions, localized electrons in d-orbitals are added to the hybrid system. No magnetic effects arising from the *d*-π interaction between these localized d-electrons and the itinerant π-electrons are detected down to 2 K, even if now the two sublattices are closer than in the salts of the nonsubstituted Keggin anions.

Finally, the most complex and original case is obtained when itinerant electrons are introduced in the inorganic magnetic anion $[PMnMo_{11}]$. In this last case a coexistence of localized and itinerant electrons is also present in the resulting mixed-valence inorganic chain. The magnetic data are indicative of antiferromagnetic pairwise interactions between Mn^{2+} ions which are more than 11 Å away. Such interaction may come from the coupling between the localized magnetic moments of Mn^{2+} ions and the itinerant "blue" electrons delocalized over all Mo sites (*d*−*d interaction*).

Acknowledgment. We thank the Spanish DGICYT for founding this work (Grant PB94-0998). J.R.G.M. thanks the Generalitat Valenciana for a predoctoral Grant. We thank the Spanish CICYT and the Generalitat Valenciana for the financial support to purchase the SQUID magnetometer.

Supporting Information Available: Labeling schemes of the structures, tables of fractional atomic coordinates, isotropic and anisotropic displacements parameters, bond lengths and angles, and the infrared band wavenumbers (cm^{-1}) and assignments in the series α_2 and α_3 $ET_8[XZM_{11}]$ (14 pages). See any current masthead page for ordering information and Web access instructions.

JA973856L